RSC Advances

PAPER

View Article Online
View Journal | View Issue

Cite this: *RSC Adv.*, 2016, **6**, 95601

Strain-induced crystallization behaviour of natural rubbers from guayule and rubber dandelion revealed by simultaneous time-resolved WAXD/tensile measurements: indispensable function for sustainable resources†

Yuko Ikeda,*[a] Preeyanuch Junkong,[b] Takumi Ohashi,[b] Treethip Phakkeeree,[b] Yuta Sakaki,[b] Atitaya Tohsan,[c] Shinzo Kohjiya[d] and Katrina Cornish[e]

Because strain-induced crystallization (SIC) behaviour is the key for predicting the performance of alternatives to *Hevea* natural rubber, characteristics of the SIC of sulfur crosslinked guayule and dandelion natural rubbers were investigated using quick *in situ* simultaneous synchrotron time-resolved wide-angle X-ray diffraction/tensile measurements, for the first time. The SIC of sulfur crosslinked *Hevea* natural rubber was also evaluated for comparison. The SIC phenomena were clearly observed when guayule and dandelion natural rubbers were purified using acetone, then crosslinked with sulfur and subjected to strain. Guayule natural rubber showed a superior SIC upon high stretching to *Hevea* natural rubber, whereas dandelion natural rubber had a similar SIC to *Hevea*. The crosslinked guayule natural rubber had larger oriented amorphous components and larger crystallite sizes parallel to the stretching direction than the crosslinked dandelion and *Hevea* natural rubbers. These characteristic features resulted in larger crystallite volumes and lower orientation fluctuations of the crystallites in guayule natural rubber than in the others. It was speculated that the differences were because of their macromolecular structures and the amounts of non-rubber components in their matrixes. However, the SIC results clearly support the fact that both guayule and dandelion natural rubbers are the real alternatives to *Hevea* natural rubber.

Received 8th September 2016
Accepted 20th September 2016

DOI: 10.1039/c6ra22455e

www.rsc.org/advances

Introduction

Guayule (*Parthenium argentatum*) and rubber dandelion (*Taraxacum kok-saghyz*, also known as the Russian dandelion, Kazakh dandelion, Buckeye Gold, TK and TKS) have long been known to produce natural rubber (NR),[1–4] and are the most promising plants for the next generation of NR sources among a large number of NR yielding plants.[5–9] Alternatives sources of NR besides the Pará rubber tree (*Hevea brasiliensis*) are related to the sustainability of our society: *Hevea* NR is an indispensable material for heavy duty tires (typically tires for aircrafts and trucks) and about 50 000 other products.[8–10] Schultes accurately and concisely summarized the history of *Hevea* NR in his paper:[11] "Few economic plants have more deeply affected civilization than the Pará rubber tree, *Hevea brasiliensis*, the product of which has made possible present day transportation and much of modern industry and technology. Furthermore, this tropical tree represents one of man's most recently domesticated plants". However, *Hevea brasiliensis*, which is cultured in rainy tropical regions, has recently experienced biosecurity problems,[8,9,12] and guayule and rubber dandelion have been greatly highlighted as possible alternative plants[5,7,9,13] because of their adaption to temperate or even subarctic zones. Lack of biodiversity of NR has long been recognized as potentially disastrous to the global rubber supply.[9,11,12,14]

The most important property of *Hevea* NR is its self-reinforcement effect, which is manifested by the strain-induced crystallization (SIC) behaviour of crosslinked NR. The *Hevea* NR is amorphous at room temperature (RT), but highly

[a]*Faculty of Molecular Chemistry and Engineering, Kyoto Institute of Technology, Matsugasaki, Sakyo, Kyoto 606-8585, Japan. E-mail: yuko@kit.ac.jp*
[b]*Graduate School of Science and Technology, Kyoto Institute of Technology, Matsugasaki, Sakyo, Kyoto 606-8585, Japan*
[c]*Department of Materials and Production Technology Engineering, Faculty of Engineering, King Mongkut's University of Technology North Bangkok, Pracharat 1 Rd, Wongsawang, Bangsue, Bangkok 10800, Thailand*
[d]*Professor Emeritus of Kyoto University, 7-506, Onawaba-cho 6, Umezu, Ukyo-ku, Kyoto 615-0925, Japan*
[e]*Departments of Food, Agricultural and Biological Engineering, and Horticulture and Crop Science, Ohio Agricultural Research and Development Center (OARDC), The Ohio State University, Wooster, OH 44691, USA*

† Electronic supplementary information (ESI) available: Details of Experimental section: FT-IR spectra of purified guayule, dandelion and *Hevea* natural rubbers and the detail of semi-quantitative analysis of those purified rubbers. See DOI: 10.1039/c6ra22455e

crystallizable upon stretching.[8,9,13,15] This property has to be evaluated during deformation *in situ* for guayule and dandelion NRs. The versatility of *Hevea* NR in industrial applications is attributed to its outstanding tensile properties and excellent crack growth resistance, which are considered to be because of its SIC ability.[9,13–22] Therefore, it is of utmost importance to thoroughly evaluate the SIC behaviour of guayule and dandelion NRs to determine their suitability as alternatives to *Hevea* NR.

Up to now, several papers on the SIC of guayule NR have been published: for example, the lower degree of crystallinity of uncrosslinked guayule NR than that of uncrosslinked *Hevea* NR was detected by using birefringence measurements.[23] Contrary to this, the degree of crystallinity was observed to become higher in guayule NR than in *Hevea* NR when both rubbers were subjected to peroxide crosslinking.[24] The SIC behaviour in the double networked guayule NR was also reported to enhance the fatigue properties when compared to the crosslinked and deproteinized *Hevea* NR.[25] However, for dandelion NR, no research on its SIC phenomenon has been reported, but the presence of crystalline reflections of uncrosslinked dandelion NR was recently found by using a wide-angle X-ray diffraction (WAXD) measurement during deformation.[26] Note that the speed of the stretching condition used in the study was very slow (1 mm min^{-1}). Therefore, the synchrotron time-resolved WAXD measurement should be applied *in situ* during fast stretching for the investigation of SIC behaviour of dandelion NR. In addition, a comparison of the SIC characteristics between the alternative NRs is necessary under the same experimental conditions for guayule NR and dandelion NR. Especially, SIC behaviors of the sulfur crosslinked rubbers should be evaluated because most of the rubber products which are used today are produced using a sulfur crosslinking reaction (vulcanization). Note that guayule NR and dandelion NR should be purified in order to remove resins from the rubbers, because the presence of resins is known to accelerate oxidation, degrade the rubber, retard the vulcanization reaction of rubber and so on.[27,28] The removal of the resins may result in productions of high quality of vulcanizates. Because the resins are insoluble in water but soluble in polar organic solvents, acetone extraction has been widely used for this purpose.[4,29–34]

In this research, guayule and dandelion NRs were subjected to acetone extraction before sulfur crosslinking. Then, the SIC behaviours of sulfur crosslinked guayule and dandelion NRs were demonstrated and directly compared to that of sulfur crosslinked *Hevea* NR under the same experimental conditions by using quick *in situ* simultaneous synchrotron WAXD/tensile measurements, for the first time.

Experimental section

Materials and purification processing

Guayule and dandelion NR latexes were extracted from mature guayule shrubs and rubber dandelion roots using alkaline aqueous extraction and purification of ground shrubs and roots, respectively.[29,35,36] The latexes were coagulated by drying at ambient laboratory conditions under gentle air flow (fume hood)[29] at The Ohio State University, Ohio Agricultural Research and Development Center (OARDC). The coagulated guayule and dandelion NRs were cut into smaller pieces, and then subjected to the conventional acetone extraction[27,29–34,37] at RT under a nitrogen atmosphere in order to remove the resins. The solvent was exchanged four times during five days. The purified rubbers were dried under vacuum first at RT and then at 40 °C to constant weight. The molecular weights of the gel free fractions of the rubbers were supposed to be $>1 \times 10^6$ g mol^{-1} as measured by one of the authors.[4,29] Commercial grade *Hevea* NR (RSS no. 1, molecular weight: $>1 \times 10^6$ g mol^{-1} (ref. 38)) was used as a reference sample and also purified similarly to the guayule and dandelion NRs.

Elemental analysis

All purified rubbers were subjected to elemental analysis before their vulcanization at the Center for Organic Elemental Microanalysis, Kyoto University in order to check the elemental compositions in the raw natural rubbers quantitatively.

Fourier-transform infrared spectroscopy (FT-IR) measurement

FT-IR measurements for purified guayule, dandelion and *Hevea* NRs were carried out at 64 scans every about 88 s in a wavenumber range from 4000 to 400 cm^{-1} at RT using a transmittance method with a Shimadzu Infrared Prestige-21. FT-IR spectra of the purified NRs are shown in Fig. S1 (ESI†). Absorption peaks for the main components, *i.e.*, hydrocarbon chains of *cis*-1,4-polyisoprenes of the three NRs were assigned: ν = 840 cm^{-1} (C–H out of plane bending in the –CH=CH– group of the *cis*-1,4-unit), 1127 cm^{-1} (CH_2 rocking), 1310 cm^{-1} (CH_2 wagging), 1375 cm^{-1} (CH_3, asymmetrical stretching), 1450 cm^{-1} (CH_2 symmetrical stretching and CH_3, asymmetrical deformation), 1664 cm^{-1} (C=C stretching), 2725 cm^{-1} (overtone of CH_3 asymmetrical deformation), 2852 cm^{-1} (CH_2 and CH_3 symmetrical stretching), 2915 cm^{-1} (CH_2 symmetrical stretching), 2959 cm^{-1} (CH_3 asymmetrical stretching), 3038 cm^{-1} (=CH stretching).[39–41] In addition to the peaks, all spectra showed specific peaks, which were attributed to each of the non-rubber components: ν = 3450 cm^{-1} (wide hydrogen bonded O–H symmetrical stretching in proteins, fatty acids and/or esters, overlapping with a small amount of environmental water absorbed by non-rubber components[39]), 1694 cm^{-1} (C=O asymmetrical stretching of dimer of acid), 1738, 1736 and 1735 cm^{-1} (C=O asymmetrical stretching of ester for the purified dandelion, *Hevea* and guayule NRs, respectively), 3280 cm^{-1} (small but relatively sharp N–H stretching of secondary amides in proteins for the purified dandelion and *Hevea* NRs), 1544 and 1622 cm^{-1} (N–H bending of mono-substituted amide II and amide I, respectively, for the purified dandelion and *Hevea* NRs), 1560 cm^{-1} (probably COO^- asymmetrical stretching of the salt for the purified guayule NR).

Preparation of NR vulcanizates

The purified rubbers were subjected to sulfur crosslinking (vulcanization): each rubber was mixed with zinc oxide at 1.0

parts per one hundred rubber by weight (phr), 2.0 phr stearic acid, 1.0 phr *N*-cyclohexyl-2-benzothiazole sulfenamide and 1.5 phr sulfur on a two-roll mill at RT. The rubber compounds obtained were cured at 140 °C in a mold to make 1 mm thick crosslinked rubber sheets. The press-heating times for guayule, dandelion and *Hevea* NRs were 15, 17 and 14 min, respectively, which were determined from the maximum torques shown in the cure curves obtained at 140 °C using the JSR Curelastometer III. Subsequently, in this paper, the sulfur crosslinked samples are designated as S-GR, S-DR and S-NR for guayule, dandelion and *Hevea* NRs, respectively. Their raw (not vulcanized but purified) rubbers are referred to as guayule NR, dandelion NR and *Hevea* NR, respectively. The network-chain densities of the crosslinked rubbers were calculated using the modified Flory–Rehner equation[42] using the results of swelling tests in toluene at 25 °C. Volume changes were measured using a OMRON VC1000 Digital Fine Scope charge coupled device (CCD) camera. The details of the swelling experiment are described in a previous paper.[43] The degrees of swelling by volume and gel fractions of S-GR, S-DR and S-NR were determined using eqn (1) and (2):

$$\text{Swelling degree by volume} = V_a/V_b \quad (1)$$

where V_b and V_a are the volumes of crosslinked sample before and after the swelling, respectively.

$$\text{Gel fraction} = W_a/W_b \quad (2)$$

where W_b is the weight of crosslinked sample before swelling and W_a is the weight of crosslinked sample after swelling and then followed by drying. The network-chain densities, degrees of swelling by volume and gel fractions of S-GR, S-DR and S-NR are summarized in Table 1.

Simultaneous WAXD/tensile measurements

Synchrotron time-resolved WAXD measurement was conducted during tensile deformation of the samples *in situ* at the BL-40XU beamline of SPring-8 in Harima, Japan. A custom made tensile tester (ISUT-2201, Aiesu Giken Co., Kyoto) was set on the beamline and WAXD patterns were recorded during both cyclic and single tensile measurements at RT. The wavelength of the X-ray was 0.08322 nm and the camera length was 131 mm. The two-dimensional (2D) WAXD patterns were recorded using a HAMAMATSU ORCA II CCD camera. The intensity of the incident X-ray was attenuated using a beamline equipped aluminum plate. The sample was exposed to the incident beam for 70 ms every 3 s in order to minimize the relaxation effect in the SIC evaluation and radiation damage to the samples during the measurements. The absorption correction for thinning of the samples under stretching was carried out using calculated correction coefficients, which were estimated on the basis of absorption coefficients per density[44] and weight fractions of each element in the samples. Ring shaped samples were used in order to correctly measure the stretching ratio (α) of the deformed samples. The inner and outer diameters of the ring shaped specimen were 11.7 and 13.7 mm, respectively. Here, α is defined as $\alpha = l/l_0$, in which l_0 is the initial length and l is the length after deformation. The stretching speed was 100 mm min^{-1}, *i.e.*, the strain speed was about 4.98 per min. The tensile experimental conditions for the uncrosslinked samples were the same as those in the simultaneous WAXD/tensile measurements for the vulcanizates although the WAXD measurements were not conducted.

WAXD analysis

The obtained WAXD images were processed using "POLAR" software (Stonybrook Technology & Applied Research, Inc.).[18,19] The WAXD patterns of stretched samples were decomposed into three components, *i.e.*, isotropic, oriented amorphous and crystalline components. The three components were integrated azimuthally within the range of ±75° from the equator. The details of this analytical method were described in previous papers by Tosaka *et al.*[18,19] Three structural parameters, "crystallinity index (CI)", "oriented amorphous index (OAI)" and "oriented index (OI)", were calculated using the following equations, and "OI" is defined as OI = CI + OAI:

$$\text{CI} = \frac{\sum_{\text{crystal}} 2\pi \int \sin\phi \mathrm{d}\phi \int I(s)s^2 \mathrm{d}s}{\sum_{\text{total}} 2\pi \int \sin\phi \mathrm{d}\phi \int I(s)s^2 \mathrm{d}s} \quad (3)$$

$$\text{OAI} = \frac{\sum_{\text{oriented-amorphous}} 2\pi \int \sin\phi \mathrm{d}\phi \int I(s)s^2 \mathrm{d}s}{\sum_{\text{total}} 2\pi \int \sin\phi \mathrm{d}\phi \int I(s)s^2 \mathrm{d}s} \quad (4)$$

Table 1 Characteristics of S-GR, S-DR and S-NR

Sample code	Network-chain density[a] × 10^5 (mol cm^{-3})	Degree of swelling by volume[b]	Gel fraction[c]	Stress at α = 4.0 (MPa)	Stress at α = 7.0 (MPa)	T_B[d] (MPa)	E_B[e]
S-GR	9.4	6.1	0.99	1.4	5.9	16.0	8.3
S-DR	9.7	5.9	0.98	1.4	7.5	16.2	8.5
S-NR	9.7	5.9	0.98	1.3	7.0	11.4	7.7

[a] Determined by using modified Flory–Rehner equation.[42] [b] Determined by the change of volume of crosslinked sample before and after swelling using eqn (1). [c] Determined by the change of weight of crosslinked sample before and after swelling using eqn (2). [d] Tensile strength at break. [e] Stretching ratio at break.

In eqn (3) and (4), $I(s)$ represents the intensity distribution of each peak that is read from the WAXD pattern, s is the radial coordinate in reciprocal space in nm^{-1} unit ($s = 2(\sin\theta/\lambda)$, where λ is the wavelength and 2θ is the scattering angle), and ϕ is the angle between the scattering vector of the peak and the fiber direction.

Coherent lengths (apparent crystallite sizes) were estimated using the Scherrer eqn (5):[45,46]

$$L_{hkl} = K\lambda/(\beta\cos\theta) \quad (5)$$

where L_{hkl} is the apparent crystallite size in the direction of the perpendicular to the (hkl) plane, and θ is the Bragg angle (half of the scattering angle). In this study, a value of 0.89 was used for K.[15,46] β was determined as follows: the intensity distribution on the equator was extracted from the original WAXD pattern, and each peak was fitted with a linear background and a Gaussian function having the form $I(x) = h\exp[-(x - x_c)^2/(2w^2)]$, where $I(x)$ is the intensity at position x, and x_c is the position at the scattering maximum. Parameters h and w are related to the peak height and peak width, respectively.[18] Each w value was converted into the half-width β.

Orientation fluctuation of 200 reflections was evaluated from the azimuthal scan of the peak:[18] the width parameter in the azimuthal direction (w_{az}) was obtained by fitting the intensity distribution with a Gaussian function. Then, w_{az} was converted into a half-width β_{az} using the following equation:

$$\beta_{az} = 2w_{az}\sqrt{-2\ln(1/2)} \quad (6)$$

Furthermore, it was reported that the value of L_{020} was approximated as $0.94L_{120}$ when an angle between the (120) and the (020) directions was nearly 19°.[47] This observation agreed well with the angle estimated by the value of lattice constants in our experimental data. Ultimately, an average volume of crystallites (V_c) is defined as follows:[47]

$$V_c = L_{200}L_{020}L_{002} = 0.94L_{200}L_{120}L_{002} \quad (7)$$

Assuming that crystallites have identical dimensions at a given stretching ratio, an average number of the crystallites per unit volume can be calculated using the V_c.[47] However, the CI value in this study was the crystallinity index. Therefore, the index of average number of the crystallites per unit volume (N) was calculated using eqn (8):

$$N = \frac{CI}{V_c} \quad (8)$$

Results and discussion

The purified guayule, dandelion and *Hevea* NRs were characterized using elemental analysis and FT-IR measurements, the results of which are summarized in Table 2. The results of acetone extraction were in good agreement with results found in previous reports.[29,48] The acetone soluble parts were much higher in the dandelion and guayule NRs than in *Hevea* NR. This is attributed to the fact that the raw dandelion and guayule NRs were collected from the plants not by tapping but by aqueous processing and followed by solvent extraction.[9] The elemental analysis showed that the percentage of H atoms of all the purified rubbers was in the same range, as shown in Table 2. However, the percentage of C atoms in dandelion NR was slightly lower than those in guayule and *Hevea* NRs. The difference in the percentage of N atoms was clearly detected among three purified NRs: the percentage of N atoms in the dandelion and *Hevea* NRs were 0.75% and 0.55%, respectively. Generally, the percentage of N determined using elemental analysis has been used for indicating the amount of proteins and phospholipids in *Hevea* NR.[49,50] Therefore, these results clearly showed that the contents of proteins and phospholipids inherent in the dandelion NR was larger than those obtained for the *Hevea* NR. However, it is worth noting that the N atom was not detected in the guayule NR (the percentage of N atom = 0), which means that this guayule NR does not contain any detectable proteins. Furthermore, the non-rubber components in the guayule, dandelion and *Hevea* NRs were evaluated using the semi-quantitative analysis of FT-IR spectra, where the relative intensity of the specific peak against the reference peak was calculated by using eqn (9):

$$\text{Relative intensity of the peak at } X \text{ cm}^{-1} = \left(\frac{\text{intensity of the peak at } X \text{ cm}^{-1}}{\text{intensity of the reference peak}}\right) \quad (9)$$

where X is 3280, 1622, 1544, 1694 and 1738 cm^{-1}, and the base lines and reference peaks for the calculation of each peak considered are described in Fig. S2 (ESI†). The relative intensities of each peak mentioned previously for the three samples are summarized in Table 2. The relative intensities of

Table 2 Characteristics of purified guayule, dandelion and *Hevea* NRs after the acetone extraction

		Elemental analysis			Relative intensity of peak[a]				
Sample	Amount of acetone soluble parts (wt%)	C (%)	H (%)	N (%)	N–H stretching	Amide I	Amide II	C=O stretching of ester	C=O stretching of dimer of acids
Purified guayule NR	14.4	86.6	11.8	0.00	N/A	N/A	N/A	0.1	0.1
Purified dandelion NR	15.6	83.9	11.7	0.75	1.3	2.9	2.2	1.0	1.3
Purified *Hevea* NR	2.6	86.0	11.6	0.55	1.1	2.5	2.0	0.5	0.6

[a] Determined using semi-quantitative analysis of FT-IR spectra using eqn (9).

absorption bands at 1694 cm^{-1} (C=O stretching (*asym*) in dimer of acids) and 1738 cm^{-1} (C=O stretching (*asym*) in ester) were larger in the order of dandelion NR > *Hevea* NR > guayule NR. Furthermore, the relative intensities of absorption bands at 3280 cm^{-1} (N–H stretching in peptide bond), 1622 cm^{-1} (amide I) and 1544 cm^{-1} (amide II) in the guayule NR were not detected using FT-IR. In addition, the dandelion NR had higher relative intensities of the absorption bands at 3280, 1622 and 1544 cm^{-1} than those of the *Hevea* NR. These results clearly suggested that the contents of proteins, fatty acids and fatty acid esters in the purified rubbers were larger in the order of dandelion NR > *Hevea* NR > guayule NR, which was in good agreement with the results obtained using elemental analysis.

Fig. 1 shows the stress–strain curves of S-GR and S-DR, where the stress–strain curves of their uncrosslinked samples before and after purification are shown together. As reported in previous studies,[30,35] the very poor tensile properties of uncrosslinked guayule and dandelion NRs without the acetone purification were also observed in this study. However, the stress of uncrosslinked guayule and dandelion NRs slightly increased after purification using acetone. The low stress of raw guayule and dandelion NRs before the acetone treatment is probably because of a plasticizing effect of resins and/or aliphatic acids inherent in NRs. It is worth noting that the sulfur crosslinking reactions using the method in this study were useful for preparing the high performance vulcanizates for guayule and dandelion NRs as shown in Fig. 1, where the substantial enhancement of tensile properties for S-GR and S-DR was obtained. The tensile stresses at $\alpha = 4$ and 7, the tensile strengths at break (T_B) and the stretching ratios at break (E_B) of S-GR, S-DR and S-NR are summarized in Table 1. It is clearly suggested that the purification and crosslinking process are essential for the raw guayule and dandelion NRs intended for use in practical applications. Characteristics of the vulcanization reaction of guayule and dandelion NRs will be reported elsewhere.

Fig. 2b shows the tensile stress–strain curves in a cycle mode measurement of the sulfur crosslinked rubbers. S-GR and S-DR were stretched up to $\alpha = 8.0$, whereas S-NR (natural rubber from *Hevea*) was stretched to $\alpha = 7.5$ because it ruptured just before $\alpha = 8.0$. Sequential changes of the WAXD pattern of each sample were observed upon stretching. Their WAXD patterns at $\alpha = 1.0$, 5.0, 8.0 or 7.5 and in retraction at $\alpha = 5.0$, 1.0 (returned to the original length) of each sample are shown in Fig. 2c. Before stretching at $\alpha = 1.0$, an amorphous halo was observed in each 2D-WAXD pattern, indicating the presence of randomly coiled amorphous chains in all samples. Upon stretching, a crystalline reflection appeared and the SIC phenomena developed in all samples. At maximum strain, all the samples showed crystalline reflection peaks together with an amorphous halo in the background. During the retracting process, the crystalline reflections decreased gradually, but the intensities in each sample remained higher than those at equivalent elongation during the stretching process. When the samples returned to $\alpha = 1.0$, their isotropic amorphous halos reverted to the relaxed states. These phenomena clearly indicate that both S-GR and S-DR show reversible SIC behaviours comparable to those observed for S-NR. These results were in agreement with the previously reported ones on the crosslinked *Hevea* NR.[18–20]

When the SIC phenomena among the samples in Fig. 2 were carefully compared, the following differences were detected: upon stretching to $\alpha = 5.0$, crystalline reflections appeared in S-DR and S-NR, but were not seen in S-GR. Furthermore, it is

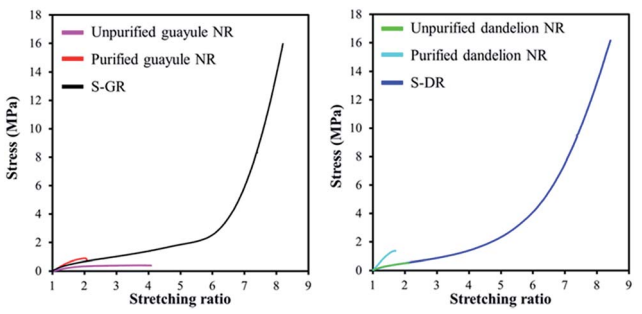

Fig. 1 Stress–strain curves of S-GR, S-DR and uncrosslinked guayule and dandelion NRs with those of uncrosslinked purified guayule and dandelion NRs. The experimental conditions for the uncrosslinked samples were the same as those in the simultaneous WAXD/tensile measurements for the vulcanizates, although the WAXD measurements were not conducted.

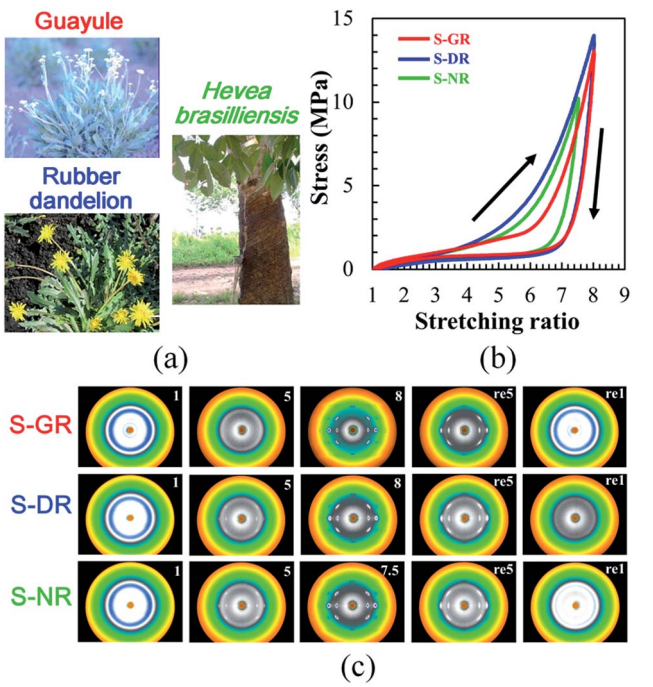

Fig. 2 (a) Photographs of guayule, rubber dandelion and *Hevea brasiliensis*: the photographs of guayule and rubber dandelion reprinted from the Source of Natural Rubber by K. Cornish, Retrieved June 13, 2016, from http://cornishlab.cfaes.ohio-state.edu/guayule. Copyright 2016 by The Ohio State University. Reprinted with permission, and *Hevea brasiliensis* photograph taken by Y. Ikeda in 2005. (b) Stress–strain curves of S-GR (—), S-DR (—) and S-NR (—). The arrows indicate the direction of deformation. (c) Sequential changes of WAXD patterns of S-GR, S-DR and S-NR in the stretching and retracting processes. Corresponding stretching ratios are indicated on the right top of the images, where "re" means the retracting process.

notable that the amorphous halo of S-GR after retraction to the original length at $\alpha = 1.0$ showed the most completely return to the original randomly coiled amorphous state of the three samples. This result was most probably related to the extremely low protein content in guayule NR, as indicated by the elemental and FT-IR analyses. The neutron scattering data in our previous paper demonstrated that the *Hevea* NR network, which contained some proteins and other compounds such as phospholipids, showed structural heterogeneity, especially localization of crosslinking points.[51] Lack of proteins and/or other effects of non-rubber components in guayule NR may have led to differences in network heterogeneity in S-GR because of the sulfur crosslinking.[43,52,53] The detail of the crosslinking reaction for guayule NR will be investigated in the near future. At least, however, the SIC apparently occurs in S-GR, thus, S-GR may be useful for the manufacture of rubber products for medical usage, because guayule NR is non-allergic.[5,7,35,54,55] Natural rubber latex allergy has been a serious problem among healthcare workers and patients, especially when using rubber gloves in surgical operations, and about 400 medical products contain NR.[5,7,38]

Further simultaneous WAXD/tensile measurements were conducted up to the mechanical rupture of the samples in Fig. 3a. The stress–strain curves were similar to those in Fig. 2b. At $\alpha \leq 4$, all the sulfur crosslinked rubbers showed comparable tensile stress as presented in the inset of Fig. 3a. Regardless of the slightly lower network-chain density of S-GR than S-DR and S-NR, slightly higher tensile stresses were observed in S-GR. This may be attributed to the better orientation capability of the network chains along the stretching direction in S-GR than the others. This is because the amount of natural crosslinked gel is much lower in guayule NR than those for dandelion and *Hevea* NRs, which are sometimes is too low for detection.[29]

In vulcanized rubber, the strain-induced crystallites are supposed to be sufficiently connected to the oriented amorphous rubber chains, to load the applied force at larger deformations.[18–20] Thus, the difference of tensile stress at the same strain among the samples is more clearly understood by relating these differences to the SIC phenomena at a high strain. Thus, the SIC parameters were determined next, in order to reveal the characteristics of the tensile properties of S-GR and S-DR using our previous methods.[19]

Variations of OI, OAI and CI values against strain are shown in Fig. 3b, c and d, respectively. The OI values tended to increase with increasing strain. It was noted that a maximum OI were around 40% in S-GR and around 30% in S-DR and S-NR, respectively. These results indicated that about 60–70% of rubber chains remained in the unoriented amorphous state, which was in agreement with the strong amorphous halo observed in Fig. 2c. Considering the three samples, only the OI values of S-GR showed a rapid initial increase, and the OI of S-GR mostly remained higher than those of the others. A similar pattern was observed in the OAI. These observations suggested that the short amorphous network chains in S-GR began to orient immediately upon stretching, as detected by the variation of the OAI. The ability of S-GR to easily and immediately orient along the stretching direction may be because of the less

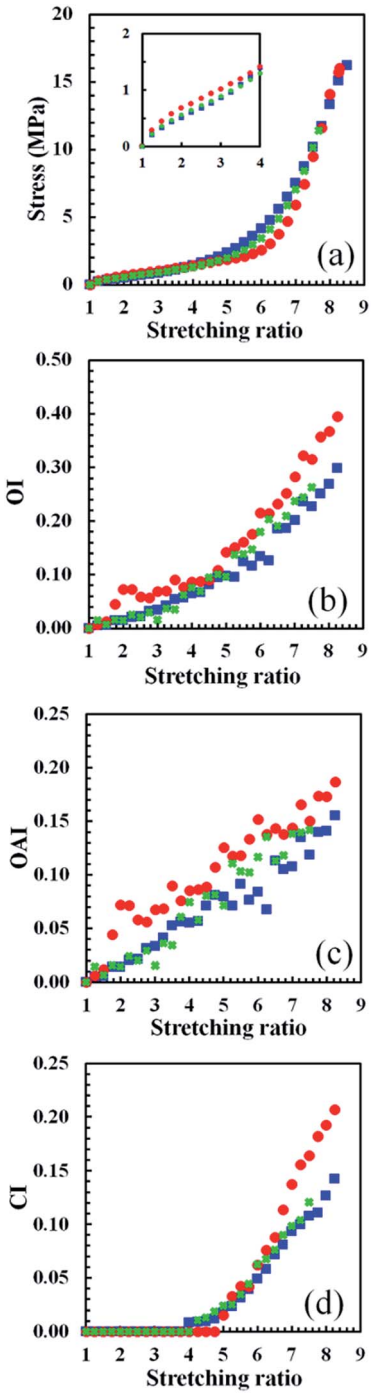

Fig. 3 (a) Stress–strain curves to the break points of S-GR (●), S-DR (■) and S-NR (✖). (b) Variations of OI, (c) OAI and (d) CI of the samples plotted against the stretching ratio.

branched polyisoprene chains in guayule NR. In fact, the main fractions of both fresh guayule NR and commercial guayule NR were reported to be a linear polymer.[56] One of the authors in this study also reported that the gel content in guayule NR was about 10% and much lower than that of *Hevea* NR.[29] Most completely return to the original randomly coiled amorphous state of S-GR shown in Fig. 2c is also explainable by this specific feature of guayule NR.

These characteristics were more clearly detected in Fig. 3d. The CI values of all the samples increased under increasing strain. Onset of SIC for S-DR, S-NR and S-GR were at $\alpha = 4.0$, 4.25 and 5.0, respectively. Although the exact reason for this behaviour is still to be determined, the order of onset strain matched the order of nitrogen content, and it was assumed that the differences in the network heterogeneity were because of the proteins. The slope, *i.e.*, the development of SIC, was highest in S-GR, whereas those of S-DR and S-NR were similar. The CI and OAI of S-GR were the highest of the three samples at $\alpha > 6$, although the tensile stresses at $5.5 < \alpha \leq 7.5$ of S-GR were lower than those of S-DR and S-NR. These differences are attributable to the presence of proteins in S-DR and S-NR, which contribute to the polymer network.

Until this research, the degrees of crystallinity for guayule, dandelion and *Hevea* NRs had been evaluated using different techniques and under different conditions, making direct comparison difficult. Without the purification, uncrosslinked guayule NR had a lower level of crystallinity than uncrosslinked *Hevea* NR as determined using on-line birefringence measurements.[23] However, the peroxide crosslinked guayule NR provided the largest degree of crystallinity with the lower onset strain of SIC than the peroxide crosslinked *Hevea* NR (SMR-10) and deproteinized *Hevea* NR, as also detected using the birefringence measurements.[24] Furthermore, uncrosslinked and unpurified dandelion NR was fully amorphous in the undeformed state, and its SIC occurred only at high strain ratios ($\alpha >$ 4) as detected by the presence of crystalline reflection in its 2D-WAXD pattern.[26] However, the results were obtained from the WAXD measurement during tensile deformation at a very slow speed of 1 mm min^{-1}. These results are useful, however, most of the SIC behaviours reported in these previous papers may have contained significant stress relaxation effects because of the non-real time WAXD measurement during stretching. In addition, other experimental details were unclear.[26] Until now, there have been no reports of simultaneous *in situ* synchrotron WAXD/tensile measurements, which were performed in the current study under large deformation and 100 times faster tensile speed (100 mm min^{-1}) than the previous report. The results reveal the SIC behaviours of S-GR, S-DR and S-NR under the same experimental conditions of quick uniaxial stretching. The SIC parameters for generated crystallites are quantitatively discussed in the next section.

Apparent crystallite sizes (coherent lengths) during stretching were determined from the WAXD profiles using the Scherrer equation.[45,46] The calculated coherent lengths are reasonably assumed to reflect actual crystallite sizes. Fig. 4a shows strain dependences of apparent lateral crystallite sizes estimated using the 200 reflection (L_{200}) for all the samples. Their L_{200} values decreased with strain and tended to be a little smaller in the samples containing proteins (S-DR and S-NR) than in S-GR, which is clearly detected to be in the early stages of SIC. The protein content may also have slightly affected crystallite size, because the L_{200} of S-DR was smaller than that of S-NR. In contrast, no differences in lateral crystallite sizes among the samples were detected using the 120 reflection (L_{120}) against the stretching ratio even in the early stages of SIC. The L_{120} values were comparable over the wide range of strain among the samples shown in Fig. 4b. There was also little decrease in L_{120} values with strain among the samples. These results suggest that more stress was perpendicularly applied to the (200) plane than to the (120) plane of the crystallites in all the samples. The smaller variation of L_{120} than of L_{200} against stretching ratio has already been reported in both sulfur and peroxide crosslinked

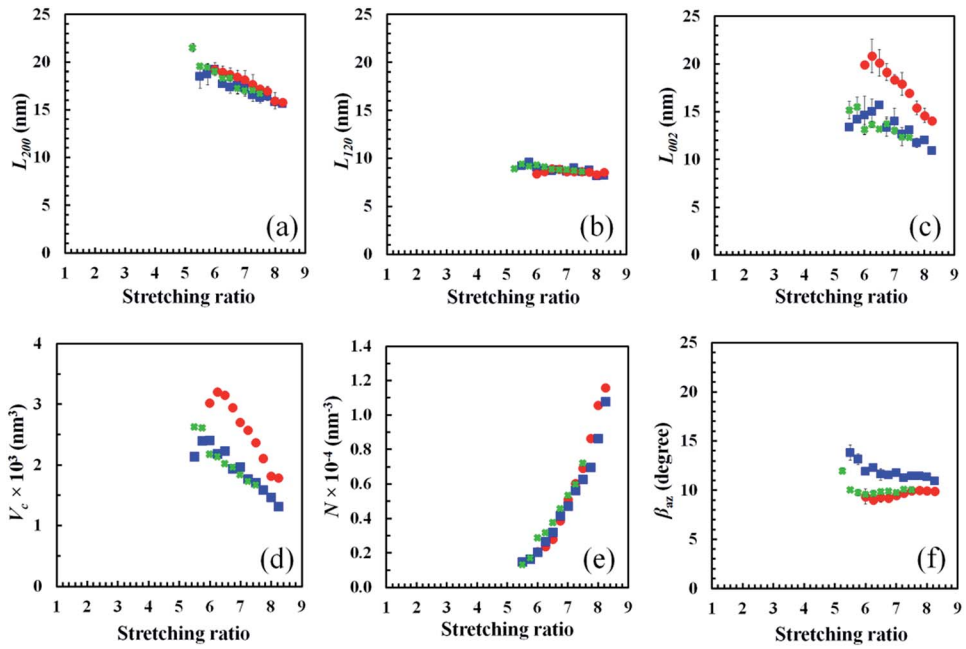

Fig. 4 Variations of apparent crystallite sizes (a) L_{200}, (b) L_{120}, (c) L_{002}, and variation of (d) average volume of crystallites, (e) indexes of average number of crystallites and (f) orientation fluctuation of crystallites for S-GR (●), S-DR (■) and S-NR (✖) plotted against the stretching ratio.

Hevea NRs in our previous work,[20] and appears to be common for the SIC behaviour of crosslinked polyisoprene segments.

The apparent crystallite sizes in the direction parallel to the stretching direction (L_{002}) of all the samples tended to increase in the beginning and decrease upon further stretching. Interestingly, however, the L_{002} values were found to be significantly different among the samples as shown in Fig. 4c: S-GR had a much larger L_{002} than S-DR and S-NR at the early stages of SIC even when the standard deviation error was considered. Because the apparent crystallite sizes perpendicular to the (002) plane are assumed to relate to the length of fully stretched chains acting as the initiating species for SIC, it is speculated that the larger the L_{002}, the longer the fully stretched chains are. Thus, the longer fully stretched chains in S-GR are attributable to the better orientation of rubber chains, which is permitted by the less branched structure of guayule NR.[56]

Using the parameters of CI and three L_{hkl} values, volumes of generated crystallites, which load the stress were calculated and compared among S-GR, S-DR and S-NR. Because of the reduction of apparent crystallite size upon stretching for all samples, their average crystallite volumes (V_c) tended to decrease with increasing stretching ratio as shown in Fig. 4d. It is worth noting that the V_c of S-GR was obviously larger than that of S-DR and S-NR at each strain. The presence of proteins in S-DR and S-NR is thought to hinder the development of SIC, whereas the less branched chemical structure of guayule NR may have promoted the development of SIC in S-GR. In addition, it was also found that the indexes of average crystallite number per unit volume (N) of S-GR, S-DR and S-NR increased with increasing strain. Although the onset strain of SIC varied in the order of S-DR < S-NR < S-GR, the indexes of N were comparable among the samples as shown in Fig. 4e. It is presumed that the physical interaction between rubber and non-rubber components accelerated the SIC at low strain for S-DR and S-NR as shown in Fig. 3d, but the physical interaction may have been broken with further stretching and followed by the formation of similar network size distributions resulting in a similar number of starting sites for SIC. Probably, the number of generated crystallites at high strain ($\alpha > 5$) for each rubber may have been mainly governed by the chemical crosslinking network. This needs to be investigated in detail.

However, the V_c and N values obtained gave a unique realisation about S-GR: the abrupt increases of tensile stress over about 6 of the stretching ratio in S-GR were mainly attributed to its larger crystallites than those of S-DR and S-NR not to the difference of crystallite number. Generally, in rubber science and technology, it has been believed that, at similar weight loadings, the smaller the filler size, the larger the filler surface area and the stronger the reinforcement effect. In this case, both the variations to the small size and to the large surface area of the filler accompany the increase of number of filler particles. However, when the number of filler particles is fixed, the filler with a bigger particle size must give a larger total surface area which leads to a better reinforcement effect than that of the

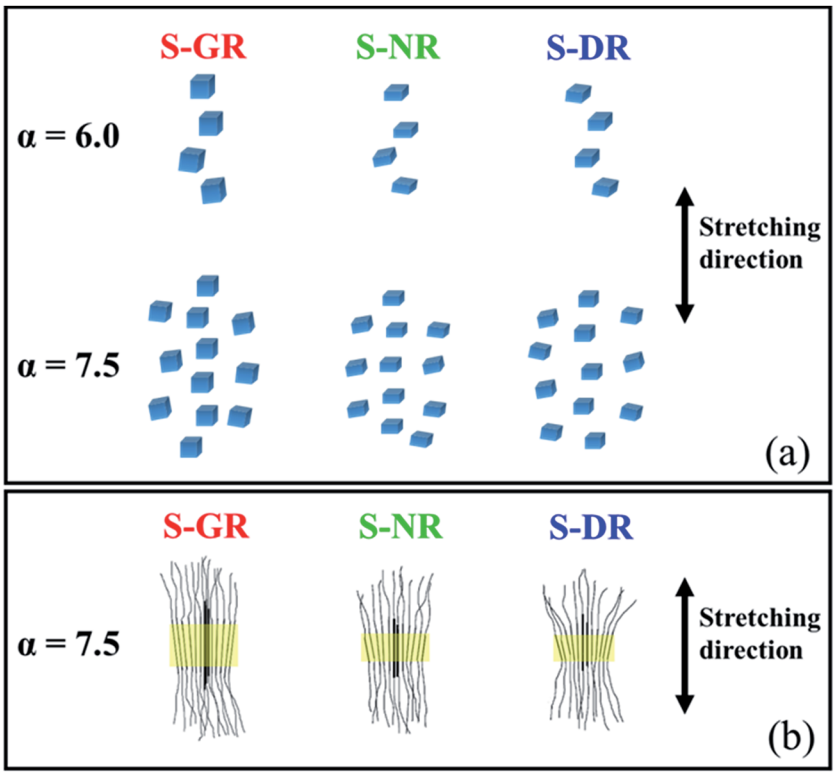

Fig. 5 (a) Schematic drawings of the morphologies at $\alpha = 6.0$ and 7.5 for the generated crystallites in S-GR, S-NR and S-DR, respectively. (b) Two-dimensional images for each generated crystallite at $\alpha = 7.5$ in S-GR, S-NR and S-DR. The yellow parts show the crystallites. Thick lines in the centers of each crystallite represent starting sites for SIC.

smaller sized ones. This scenario agrees well the results of this study: the larger crystallites generated connected with the larger oriented amorphous chains in S-GR can load the stress better than the smaller crystallites in S-DR and S-NR. Up to now, the scenario has been accepted intuitively among the rubber scientists and technologists. However, the control of the number of filler particles has been difficult, because of the aggregation of filler particles, and by the lack of experimental evidence. Therefore, the results in this study will be useful for the design of materials of soft nanocomposites mixed with nano-fillers. Additionally, of course, the influence of orientation of crystallites has to be taken into account to explain the reinforcing effect of the strain-generated crystallites, which is discussed in the next section.

The orientation fluctuation of crystallites (β_{az}) also plays a role in the abrupt increase of stress in S-GR as mentioned before. Fig. 4f shows the strain dependence of β_{az} for all samples. The smaller the value of β_{az}, the smaller fluctuations in orientation. As shown in Fig. 4f, the orientation of crystallites along the stretching direction was significantly disturbed at the low strain for all samples, but the fluctuation degree decreased and became almost similar upon further stretching. This may be because of the balancing of the perturbation of the stretched chains by the increase of number of crystallites, with the better chain orientation caused by the decreased crystallite size. However, at a given stretching ratio, considering to the standard deviation error, the orientation fluctuation of crystallites in S-DR was much larger than that in S-NR, and probably corresponds to the higher N content. The proteins in the matrixes of S-DR are supposed to prevent significantly the orientation of crystallites because of the steric hindrance. Unexpectedly, S-GR exhibited a slightly lower β_{az} than S-NR even with 0% N content. This is attributable to the competitive effects between the increase of β_{az} because of the large crystallite size in S-GR and the good alignment of the crystallites to the stretching direction because of the less branched chain molecular structure of guayule NR.

As a result, the lower orientation fluctuation of crystallites in S-GR seems to be an important factor in addition to the larger apparent crystallite size and higher OAI, affecting the reinforcement of S-GR, and causing the abrupt increase of tensile stresses at $\alpha > 6$ for S-GR. The speculated orientation behaviours of the crystallites in S-GR, S-DR and S-NR are illustrated in Fig. 5.

Conclusion

The SIC of sulfur crosslinked guayule and dandelion NRs were clearly detected using the quick time-resolved simultaneous synchrotron WAXD measurement during tensile deformation *in situ* for the first time, where the natural rubbers were purified by acetone, followed by sulfur crosslinking. The detailed investigation revealed that the SIC of NR from guayule was significantly more pronounced at high strain than that of *Hevea brasiliensis*: the onset of SIC occurred more slowly, but the development of SIC became faster and the crystallites generated became larger and its orientation was more aligned to the stretching direction in guayule NR than the other rubbers. The differences are attributed to their macromolecular structures and the amounts of non-rubber components in their matrixes. However, the SIC behaviour of NR from rubber dandelion was comparable with that of *Hevea brasiliensis*. The SIC, which is an indispensable function and absolutely required for alternatives to *Hevea* NR as a sustainable resource,[13] was accurately revealed in both guayule and dandelion NRs in this study.

Acknowledgements

This work was supported by JST ALCA program (2015) to Y. I. The WAXD experiment was performed at the BL-40XU in the SPring-8 with the approval of the Japan Synchrotron Radiation Research Institute (JASRI) (Proposal No. 2015A1872, 2015B1814).

Notes and references

1 F. E. Lloyd, *Guayule (Parthenium argentatum gray): A Rubber-Plant of the Chihuahuan Desert*, Carnegie Institution of Washington, Washington D.C., 1911.
2 W. W. Gordon and B. J. Stevenson, *Russian Dandelion (KOK-SAGHYZ): An Emergency Source of Natural Rubber*, U. S. Department of Agriculture, Washington D. C., 1947.
3 National Academy of Sciences, *Guayule: An Alternative Source of Natural Rubber*, Books for Business, New York, 2002, Originally published in 1977.
4 J. B. van Beilen and Y. Poirier, *Crit. Rev. Biotechnol.*, 2007, **27**, 217–231.
5 H. Mooibroek and K. Cornish, *Appl. Microbiol. Biotechnol.*, 2000, **53**, 355–365.
6 M. R. Finlay, *Growing American Rubber: Strategic Plants and the Politics of National Security*, Rutgers University Press, New Brunswick, 2009.
7 K. Cornish, in *Chemistry, Manufacturing and Applications of Natural rubber*, ed. S. Kohjiya and Y. Ikeda, Woodhead Publishing, Cambridge, 2014, ch. 1, pp. 3–29.
8 S. Kohjiya, *Natural Rubber: From the Odyssey of Hevea Tree to the Age of Transportation*, Smithers Rapra Publications, Shrewsbury, 2015.
9 Y. Ikeda, A. Tohsan and S. Kohjiya, in *Sustainable Development Processes, Challenges and Prospects*, ed. D. Reyes, Nova Science Publishers, New York, 2015, ch. 3, pp. 65–85.
10 Y. Hirata, H. Kondo and Y. Ozawa, in *Chemistry, Manufacturing and Applications of Natural rubber*, ed. S. Kohjiya and Y. Ikeda, Woodhead Publishing, Cambridge, 2014, ch. 12, pp. 325–352.
11 R. Schultes, *Bot. Rev.*, 1970, **36**, 197–276.
12 M. J. W. Cock, M. Kenis and R. Wittenberg, *Natural Rubber: Biosecurity and Forests: An Introduction*, Rubber Forestry Department, Food and Agricultural Organization (FAO) of the United Nations, Rome, 2003.
13 A. H. Tullo, Guayule Gets Ready to Hit the Road, *Chem. Eng. News.*, 2015, 18–19.

14 P. J. George and J. C. Kuruvilla, *Natural Rubber: Agromanagement and Crop Processing*, Rubber Research Institute of India, Kottayam, 2000.
15 S. Murakami, K. Senoo, S. Toki and S. Kohjiya, *Polymer*, 2002, **43**, 2117–2120.
16 S. Toki, I. Sics, S. Ran, L. Liu, B. S. Hsiao, S. Murakami, K. Senoo and S. Kohjiya, *Macromolecules*, 2002, **35**, 6578–6584.
17 S. Trabelsi, P. A. Albouy and J. Rault, *Macromolecules*, 2002, **35**, 10054–10061.
18 M. Tosaka, S. Murakami, S. Poompradub, S. Kohjiya, Y. Ikeda, S. Toki, I. Sics and B. S. Hsiao, *Macromolecules*, 2004, **37**, 3299–3309.
19 M. Tosaka, S. Kohjiya, S. Murakami, S. Poompradub, Y. Ikeda, S. Toki, I. Sics and B. S. Hsiao, *Rubber Chem. Technol.*, 2004, **77**, 711–723.
20 Y. Ikeda, Y. Yasuda, K. Hijikata, M. Tosaka and S. Kohjiya, *Macromolecules*, 2008, **41**, 5876–5884.
21 S. Toki, in *Chemistry, Manufacturing and Applications of Natural rubber*, ed. S. Kohjiya and Y. Ikeda, Woodhead Publishing, Cambridge, 2014, ch. 5, pp. 135–167.
22 K. Bruning, *In situ Structure Characterization of Elastomers during Deformation and Fracture*, Springer, Heidelberg, 2014.
23 Y. Shimimura, J. L. White and J. E. Spruiell, *J. Appl. Polym. Sci.*, 1982, **27**, 3553–3567.
24 I. S. Choi, *Rubber Chem. Technol.*, 1997, **70**, 202–210.
25 P. G. Santangelo and C. M. Roland, *Rubber Chem. Technol.*, 2003, **76**, 892–898.
26 S. Musto, V. Barbera, M. Maggio, M. Mauro, G. Guerra and M. Galimberti, *Polym. Adv. Technol.*, 2016, **27**, 1082–1090.
27 L. F. Ramos-De Valle, *Rubber Chem. Technol.*, 1981, **54**, 24–33.
28 J. M. Slon, M. J. Magliochetti and W. X. Zukas, *Rubber Chem. Technol.*, 1986, **59**, 800.
29 C. McMahan, D. Kostyal, D. Lhamo and K. Cornish, *J. Appl. Polym. Sci.*, 2015, **132**, 42051(1)–42051(7).
30 M. E. Salvucci, T. A. Coffelt and K. Cornish, *Ind. Crops Prod.*, 2009, **30**, 9–16.
31 L. F. Ramos de Valle and M. Montelongo, *Rubber Chem. Technol.*, 1978, **51**, 863–871.
32 L. T. Black, G. E. Hamerstrand, F. S. Nakayama and B. A. Rasnik, *Rubber Chem. Technol.*, 1983, **56**, 367–371.
33 T. F. Banigan, A. J. Verbiscar and T. A. Oda, *Rubber Chem. Technol.*, 1982, **55**, 407–415.
34 W. W. Schloman, *Ind. Crops Prod.*, 2005, **22**, 41–47.
35 W. W. Schloman Jr, F. Wyzgoski, D. Mcintyre, K. Cornish and D. J. Siler, *Rubber Chem.Technol.*, 1996, **69**, 215–222.
36 R. K. Eskew and P. W. Edwards, *US* 2,393,035, 1946.
37 N. T. Thuong, O. Yamamoto, P. T. Nghia, K. Cornish and S. Kawahara, *Polym. Adv. Technol.*, 2016, in press.
38 M. Morton, *Rubber Technology*, Ohio, USA, 3rd edn, 1999.
39 L. Xu, C. Huang, M. Luo, W. Qu, H. Liu, Z. Gu, L. Jing, G. Huang and J. A. Zheng, *RSC. Adv.*, 2015, **5**, 91742–91750.
40 D. Chen, H. Shao, W. Yao and B. Huang, *Int. J. Polym. Sci.*, 2013, 937284.
41 M. Hesse, H. Meier and B. Zeeh, *Spectroscopic methods in organic chemistry*, Thieme, Stuttgart, New York, 2nd edn, 2008.
42 P. J. Flory, *J. Chem. Phys.*, 1950, **18**, 108–111.
43 Y. Ikeda, N. Higashitani, K. Hijikata, Y. Kokubo, Y. Morita, M. Shibayama, N. Osaka, T. Suzuki, H. Endo and S. Kohjiya, *Macromolecules*, 2009, **42**, 2741–2748.
44 T. Hahn, in *International Tables for Crystallography*, D. Reidel Pub. Co., Holland, 1983, vol. A, p. 157.
45 P. Scherrer, *Nachr. Ges. Wiss. Goettingen, Math.-Phys. Kl.*, 1918, **2**, 98–100.
46 H. P. Klug and L. E. Alexander, in *X-ray Diffraction Procedures for Polycrystalline and Amorphous Materials*, Wiley-Interscience, New York, 2nd edn, 1974, pp. 687–692.
47 N. Candau, R. Laghmach, L. Chazeau, J. M. Chenal, C. Gauthier, T. Biben and E. Munch, *Macromolecules*, 2014, **47**, 5815–5824.
48 A. U. Buranov and B. J. Elmuradov, *J. Agric. Food Chem.*, 2010, **58**, 734–743.
49 J. Sansatsadeekul, J. Sakdapipanich and P. Rogruthai, *J. Biosci. Bioeng.*, 2011, **111**, 628–634.
50 R. M. B. Moreno, M. Ferreira, P. S. Gonçalves and L. H. C. Mattoso, *Sci. Agric. (Piracicaba, Braz.)*, 2005, **62**, 122–126.
51 T. Karino, Y. Ikeda, Y. Yasuda, S. Kohjiya and M. Shibayama, *Biomacromolecules*, 2007, **8**, 693–699.
52 Y. Yasuda, S. Minoda, T. Ohashi, H. Yokohama and Y. Ikeda, Macromol. Chem. Phys., 2014, **215**, 971–977.
53 Y. Ikeda, Y. Yasuda, T. Ohashi, H. Yokohama, S. Minoda, H. Kobayashi and T. Honma, *Macromolecules*, 2015, **48**, 462–475.
54 D. J. Siler and K. Cornish, *Ind. Crops Prod.*, 1994, **2**, 307–313.
55 T. Palosuo, in *Chemistry, Manufacturing anplications of Natural rubber*, ed. S. Kohjiya and Y. Ikeda, Woodhead Publishing, Cambridge, 2014, ch. 18, pp. 452–474.
56 T. Hager, A. Macarthur, D. Mcintyre and R. Seeger, *Rubber Chem. Technol.*, 1979, **52**, 693–709.

